Available online at www.sciencedirect.com
ScienceDirect
International Journal of Mass Spectrometry 260 (2007) 203–211
International Journal of Mass Spectrometry
www.elsevier.com/locate/ijms

High-resolution MALDI imaging mass spectrometry allows localization of peptide distributions at cellular length scales in pituitary tissue sections

A.F. Maarten Altelaar [a], Ioana M. Taban [a], Liam A. McDonnell [a], Peter D.E.M. Verhaert [b], Robert P.J. de Lange [c], Roger A.H. Adan [c], Wolter J. Mooi [d], Ron M.A. Heeren [a,*], Sander R. Piersma [a,1]

[a] *FOM Institute for Atomic and Molecular Physics, Kruislaan 407, 1098 SJ Amsterdam, The Netherlands*
[b] *Analytical Biotechnology, Department of Biotechnology, Technical University Delft, Julianalaan 67, 2628 BC Delft, The Netherlands*
[c] *Rudolf Magnus Institute of Neuroscience, Department of Pharmacology and Anatomy, University Medical Center Utrecht, Universiteitsweg 100, 3584 CG Utrecht, The Netherlands*
[d] *Department of Pathology, Free University Medical Centre, De Boelelaan 1117, 1081 HV Amsterdam, The Netherlands*

Received 19 July 2006; received in revised form 22 September 2006; accepted 22 September 2006
Available online 27 October 2006

Abstract

Matrix assisted laser desorption/ionization (MALDI) imaging mass spectrometry (IMS) has been used to determine peptide distributions directly from rat, mouse and human pituitary tissue sections. Since these organs are small (10^2–10^3 μm) the spatial resolution of IMS is a key issue in molecular imaging of pituitary tissue sections. Here we show that high-resolution IMS allows localization of neuropeptide distributions within different cell clusters of a single organ of a pituitary tissue section. The sample preparation protocol does not result in analyte redistribution and is therefore applicable to IMS experiments at cellular length scales. The stigmatic imaging mass spectrometer used in this study produces selected-ion-count images with pixel sizes of 500 nm and a resolving power of 4 μm, yielding superior spatial detail compared to images obtained in microprobe imaging experiments. Furthermore, we show that with imaging mass spectrometry a distinction can be made between different mammalian tissue sections based on differences in the amino acid sequence of neuropeptides with the same function. This example demonstrates the power of IMS for label-free molecular imaging at relevant biological length scales.

Keywords: Imaging MS; MALDI; Tissue; Neuropeptide; Dataprocessing

1. Introduction

Imaging mass spectrometry (IMS) has proven to be a powerful tool in the investigation of molecular distributions in both healthy and diseased tissue [1–6]. Matrix assisted laser desorption/ionization (MALDI) MS has shown to produce peptide and protein signals directly from tissue sections [1,2,6,7]. As in any imaging technique the obtainable spatial resolution is a key issue. Our current aim is to obtain cellular resolution, without compromising the original spatial distributions of the molecules of interest. In IMS, this has so far been limited by both instrumentation and sample preparation issues. In conventional microprobe MALDI-IMS the obtainable spatial resolution is determined by a combination of the laser spotsize and the sample preparation technique. Typically, the laser spotsize in MALDI-IMS ranges from ∼50 to 200 μm. The spatial resolution of MALDI imaging has been increased by developing optical lenses, able to focus the laser to submicron dimensions [8]. However, it has been shown that the sensitivity of MALDI for high mass molecules decreases significantly with decreasing spot size (two orders of magnitude for spot sizes of ≈7 μm diameter) [9].

Recently, a new approach to MALDI imaging has been developed in our group: the stigmatic mass microscope [6,10]. In this instrument the obtainable spatial resolution is independent from the size of the desorption/ionization area. The desorbed ions

* Corresponding author. Tel.: +31 20 6081234; fax: +31 20 6684106.
E-mail address: heeren@amolf.nl (R.M.A. Heeren).
[1] Present address: Oncoproteomics Laboratory, Free University Medical Centre, De Boelelaan 1117, 1081 HV Amsterdam, The Netherlands.

1387-3806/$ – see front matter © 2006 Elsevier B.V. All rights reserved.
doi:10.1016/j.ijms.2006.09.028

within a large laser spot (150 μm × 200 μm) retain their original spatial distribution during time-of-flight (ToF) separation and are detected by a position sensitive detector. The resulting stigmatic images at highest magnification have a pixel size of 500 nm and a resolving power of 4 μm, both for UV and IR lasers [10,11]. With the mass microscope we approach the spatial resolution obtained by secondary ion mass spectrometry (SIMS) but with the ability to desorb large organic molecules like peptides and proteins. In addition, this high spatial resolution is obtained with much higher speed of analysis [10].

In order to benefit from this high spatial resolution, the preparation of the tissue sections before MALDI analysis is of crucial importance. The goal is to obtain sufficient peptide and protein signal intensity from matrix crystals smaller than the tissue features of interest and without redistribution of the analyte molecules. One method of improving signal intensity is washing of the tissue sections. If no washing step is performed before addition of the MALDI matrix, the physiological saline hampers the crystallization of the MALDI matrix. When a washing step is performed the crystallization of the matrix on the tissue results in more uniform and smaller sized crystals, but diffusion of the molecular content has to be limited as much as possible. The addition of the matrix itself can also determine the maximum obtainable spatial resolution. If the matrix is added in droplets as in piezodispensing or in acoustic deposition [12], the size of the droplets, and thus the maximum obtainable spatial resolution, is in the order of 150–250 μm. Other approaches to matrix deposition like electrospray or pressure driven deposition result in much smaller matrix crystals (∼0.5–1 and 1–10 μm, respectively), but smaller crystals can compromise sensitivity in MALDI-MS.

The tissue size and the morphological length scales will ultimately determine the spatial resolution needed in IMS. The first direct MALDI-MS analysis of peptides from dissected cells was already performed over a decade ago [13,14], followed by the first example of profiling of peptides in rat pituitary tissue, by Caprioli et al. [15] in 1997.

The pituitary gland is a small organ at the base of the brain, connected to the hypothalamus. The pituitary is part of the endocrine signaling system and secretes hormones into the circulatory system. The primary function of the pituitary gland is regulation of the endocrine system itself by controlling the function of the other glands in the endocrine system. The action of the pituitary is regulated by signals coming from the hypothalamus. In endocrine signaling a high concentration of hormones (e.g., neuropeptides) are secreted in a burst-like manner. The high neuropeptide content in the pituitary gland makes the organ an excellent model for analysis with IMS.

The pituitary is made up of two different regions called the adenohypophysis (or anterior and intermediate lobe) and the neurohypophysis (or posterior lobe) [16]. The cells of the anterior lobe synthesize and secrete at least seven peptide hormones associated with growth, development, metabolism, and sexual function. The intermediate lobe synthesizes and releases specific peptide products from the pro-opiomelanocortin (POMC) precursor protein, among which is the well characterized α-melanocyte stimulating hormone (MSH). The posterior pituitary does not synthesize but only stores and secretes the peptides vasopressin and oxytocin, derived from the ProVP and ProOX precursors, respectively. These peptides are synthesized in the paraventricular and supraoptic nuclei of the hypothalamus and subsequently transported and stored in the posterior lobe [16–18]. We recently showed the localization of the peptide vasopressin in the hypothalamic area using imaging MS [6].

Here we use imaging MALDI-MS to study the peptide distributions in pituitary tissue of rat, mouse and human. We show that both improved instrumentation and sample preparation protocols allow mapping of neuropeptide distributions at high spatial resolution, showing features at cellular length scales.

2. Experimental

2.1. Materials

α-Cyano-4-hydroxycinnamic acid (HCCA), 2,5-dihydroxybenzoic acid (DHB) trifluoracetic acid (TFA) and HPLC grade water were purchased from Sigma–Aldrich (Zwijndrecht, The Netherlands). Ethanol was purchased from Biosolve (Valkenswaard, The Netherlands).

2.2. Tissue sections

2.2.1. Rat

Experimental procedures were in accordance with the European directives (86/609/EEC) and approved by the Commission on Laboratory Animal Experiments of the University Medical Centre Utrecht. Male Wistar rats (Crl:WU) weighing 350 g were obtained from Charles River (Germany). Rats were decapitated without prior anesthesia and pituitary glands were dissected and frozen in liquid isopentane, cooled to −50 °C on dry ice and then stored at −80 °C until sectioning.

2.2.2. Mouse

Juvenile male mice were decapitated without prior anesthesia and pituitary glands were dissected and frozen and stored in ethanol, cooled to −45 °C, until sectioning.

2.2.3. Human

Normal pituitary glands were obtained at autopsy from individuals who had died of unrelated causes, and whose pituitary glands showed normal growth features. The tissue was snap frozen in liquid nitrogen and stored at −70 °C.

Ten micrometers thick pituitary tissue sections were cut from all species using a cryomicrotome at −17 °C. Sections were thaw-mounted on ITO-coated glass slides and were stored at −80 °C until use. Prior to mass spectrometry, tissue sections were brought to room temperature in a desiccator over a silica gel canister (1 h).

2.3. Sample preparation

After drying, both rat and human pituitary tissue sections were washed twice for 1 min in ice-cold 70% ethanol and dried at room temperature [19]. Mouse pituitary tissue sections were

not washed before matrix deposition. In the case of the human pituitary tissue sections, adjunct sections were haematoxylin and eosin (H&E) stained to check and compare morphological features. A TLC sprayer (Sigma–Aldrich, Zwijndrecht, The Netherlands) was used to spray the matrix solution, 10 mg/ml HCCA or 40 mg/ml DHB in 50% EtOH/0.1% TFA, for MALDI-MS. The nitrogen pressure required for efficient nebulisation was 0.3–0.4 bar. Four nanometers of gold was sputter coated on the sample surface using a Quorum Technologies (Newhaven, East Sussex, UK) SC7640 sputter coater equipped with a FT7607 quartz crystal microbalance stage and a FT7690 film thickness monitor.

2.4. Imaging mass spectrometry

MALDI stigmatic imaging MS was performed on an extensively modified Physical Electronics (Eden Prairie, MN) TRIFT-II (triple focusing time-of-flight) mass spectrometer equipped with a phosphor screen/CCD camera optical detection combination as described in detail by Luxembourg et al. [10] The ion-optics of this mass spectrometric microscope have been designed such that a magnified (ion-optical) image of the surface is mapped onto a two-dimensional detector [20]. In short, a custom-designed interface was constructed that controls the size, position and homogeneity of the UV laser spot. It consists of an ultrahigh vacuum compatible microscope objective (LMU-5X-NUV, Optics For Research) with a focal length of 40 mm. This is mounted on a telescopic and maneuverable UHV flange for use with a wedge, diode pumped solid-state Nd-YAG laser source, at 355 nm wavelength and 2 ns pulse duration (BrightSolutions, Italy). The desorbed ions are extracted through a 3.2 keV electric field into the ToF analyzer and post-accelerated by an additional 9 kV prior to detection on a 1-in. diameter dual microchannel plate (DMCP) phosphor screen detector assembly (APD 30 25 12/10/12 PS I EDR 60:1 P-20 MgO-coated, Burle Industries GmbH, Baesweiler, Germany) located in the instrument's final image plane. Mass spectra are obtained from the MCP detector after which ion images are formed on the phosphor screen and projected onto a CCD camera with 9.9-μm pixel size (Imager 3, La Vision, Goettingen, Germany) by a zoom lens (Thales Optem, Fairport, NY) that reduces the image size to fit the CCD chip. High-speed ion blankers are used to control ions which reach the detector. The total magnification obtained in the MALDI-ion microscope is determined by an ion-optical and a light-optical component. Depending on the settings of the instrument, images were recorded with 10× or 20× overall magnification, resulting in images pixel sizes of 1 μm and 500 nm, respectively.

Single-shot 200 μm total-ion-count (TIC) MALDI stigmatic images were acquired and stored as tagged image file format (tiff) files with the corresponding synchronized ADC signals (Acqiris, Geneva, Switzerland). To image an entire pituitary tissue section individual linescans were acquired by moving the sample stage at 100 μm/s while continuously firing the laser with a repetition rate of 10 Hz. At the end of the linescan (i.e., tissue section) the stage was stepped in the *y* direction by 80, 100 or 120 μm increments. This process was repeated as many times as required to image the entire tissue section.

2.5. Mass spectrometry

Electrospray-MS was performed on a quadrupole ToF Q-ToF 2 instrument (Micromass, Manchester, UK) coupled online with a capillary HPLC (CapLC) (Waters, Milford, MA, USA). Peptides were separated on a capillary C18 reversed-phase column (75 μm i.d., 15 cm L) (LC Packings, Amsterdam, The Netherlands) using a 5–60% acetonitrile gradient in 0.1% formic acid (80 min; 200 nL/min). The column was connected to a metal-coated fused-silica electrospray needle (tip i.d., 10 μm) (NewObjective, Woburn, MA, USA).

FTICR-MS experiments were performed on a 7 T Bruker Daltonics Apex III equipped with a nitrogen laser (337 nm). At each position, the ions generated from 10 laser shots were accumulated in an external hexapole ion trap and then transferred to the ICR cell for detection or tandem mass spectrometry.

2.6. MALDI data processing

Software was developed in-house to align all overlapping single-shot images into a linescan, and subsequently all linescans into an image. This high-resolution TIC image (pixel size 500 nm, resolving power ∼4 μm) was overlaid with the course resolution ADC data at each position. For comparison purposes the ADC image data was digitally resampled at different pixel sizes and treated like regular microprobe data.

3. Results

3.1. High-resolution IMS

Fig. 1 shows a schematic representation of the different protocols used to obtain high-resolution MS images. In stigmatic imaging the obtainable spatial resolution is not dependent on the size of the laser spot but depends on the quality of the ion-optics. After irradiation by the 150 μm × 200 μm homogeneous laser pulse the desorbed ions pass an immersion lens/transfer lens combination followed by a high-speed blanker. Subsequently time-of-flight separation takes place. Three semi-hemispherical electrostatic analyzers (ESA) are integral part of the 2-m flight path and are responsible for up to 200 eV kinetic energy compensation. After the third ESA the ions pass a second high-speed blanker which, in combination with the first high-speed blanker, can be used for selected ion imaging. All ions desorbed from the tissue surface preserve their original spatial distribution during time-of-flight separation and are depicted at a position sensitive detector. This allows the simultaneous recording of a microscope and microprobe dataset is a single experiment. The position sensitive detector consists of a CCD camera phosphor screen assembly, where snapshots of the ions reaching the phosphor screen are taken (Fig. 1A). These snapshots are used to construct the stigmatic ion images while at the same time the acquired *m/z* data can be used to construct course resolution microprobe ion images. In order to construct whole tissue images a linescan is taken over the entire tissue section, by moving the sample stage at a constant speed (typically 100 μm/s) under a continuously firing laser. At the end of

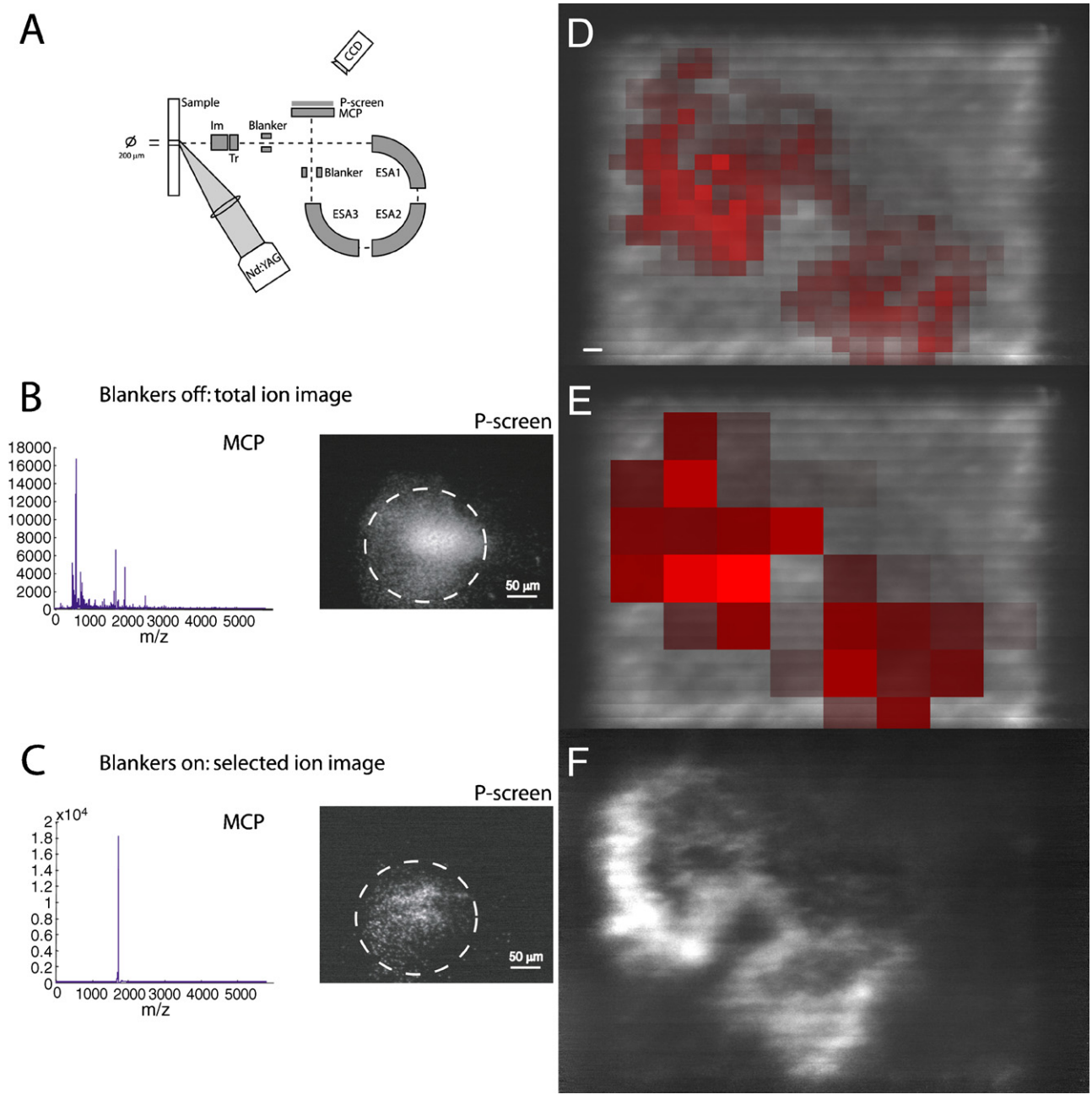

Fig. 1. Instrumentation of the stigmatic mass microscope and a comparison with microprobe IMS. (A) Schematic representation of the Physical Electronics Trift II mass spectrometer; (B) TIC and (C) stigmatic single ion imaging. The distribution of the neuropeptide α-MSH (diacetylated) in microprobe imaging, depicted with a resampled pixel size of (D) 80 μm × 80 μm (red) and (E) 250 μm × 250 μm (red) and overlaid on the stigmatic TIC image, is compared to (F) the stigmatic ion image of diacetylated-α-MSH. Scale bar is 100 μm.

a linescan the sample stage is moved upwards by 40–60% of the laser spotsize and another linescan is taken, until the entire tissue section is measured. With in-house developed software the stigmatic ion images are stitched together to form a linescan. These individual linescans are then combined to form the TIC image of the entire tissue section (Fig. 1B). The in-house developed software calculates the overlap of the consecutive laser shots and adds the intensity data of the overlapping areas in the images. As can be seen in Fig. 1C, the TRIFT high-speed blankers can be used to record stigmatic selected ion images. In this case the high-speed blankers are used to remove all ions except the ones passing through a ∼3 μs time window, which is set manually. In the mass spectrum a single isolated peak can be seen at the selected *m/z* position. Since only this single ion reaches the position sensitive detector, high spatial resolution mass resolved selected-ion-count (SIC) images can be created.

Fig. 1D–F shows the localization of the neuropeptide α-MSH in mouse pituitary tissue. The images in Fig. 1D and E shows a microscope mode TIC image (gray) in the background overlaid with microprobe mode SIC image constructed from the MCP *m/z* data of diacetylated (diAc) α-MSH (red). In order

to record the TIC image of the entire tissue section, 25 individual linescans were acquired with intervals of 80 μm, resulting in 10 μm × 80 μm pixels. To compare the obtainable spatial resolution in the conventional microprobe mode versus the microscope mode Fig. 1D and E is depicted with a digitally resampled 80 μm × 80 μm (Fig. 1D) and 250 μm × 250 μm (Fig. 1E) spatial resolution, the latter one representing the spatial resolution used in recent MALDI imaging literature [5]. In this figure it can be clearly seen that the spatial resolution obtained with the conventional approach is too low to be able to localize neuropeptides within tissue features at cellular length scales. Fig. 1E shows a selected ion microscope mode image of the same tissue section. Here, the distribution of the diAc-α-MSH ion is imaged, blanking all other ions desorbed, as can be seen in the corresponding mass spectrum in Fig. 1C. The diAc-α-MSH ions pass through the ToF mass spectrometer and form an ion-optical image at the position sensitive detector, comparable to wide field optical microcopy. Since the diAc-α-MSH ions original spatial orientation at the surface of the tissue is not disturbed during ToF analysis the image depicted at the position sensitive detector is a true reflection of this spatial orientation, showing spatial detail from within the laserspot. In this manner molecular images can be obtained with pixel sizes of 500 nm and a spatial resolving power of 4 μm. The comparison of this image with the ones in Fig. 1D and E, demonstrates that the microscope mode approach delivers superior spatial detail.

3.2. Sample preparation

The precise localization of neuropeptides in pituitary tissue sections by IMS requires a robust sample preparation technique. To perform direct tissue MALDI-IMS, multiple approaches can be utilized. First there is the choice whether to wash the tissue sections. If no washing step is performed the physiological conditions of the tissue hamper the crystallization of the MALDI matrix. In this case DHB is used as matrix because of its tolerance to high salt loads. Washing the sample results in uniform crystallization of the matrix on top of the tissue, irrespective of the chosen matrix, but holds the possibility of diffusion or washing out of the molecules of interest. After washing HCCA can be added as matrix in several spray cycles, which result in much smaller crystal sizes than DHB. Because of these small matrix crystals this technique is better suited for high spatial resolution imaging. In order to prevent diffusion of the peptides as much as possible the tissue sections are immersed in 70% ice-cold ethanol, while producing a minimal amount of movement of the solvent. The tissue sections are left in this first solution for 1 min without further movement and are subsequently transferred to the second 70% ice-cold ethanol solution for another wash step, taking the same precautions. In the study of the mouse pituitary sections no washing step was performed and concentrated DHB solution (40 mg/ml) was sprayed directly on the tissue surface. The DHB matrix still crystallizes on the tissue surface but distinct differences between the crystals on and adjacent to the tissue surface can be seen. The crystals formed adjacent to the tissue are much more translucent, spiked and differ a lot in size while the crystals on the surface of the tissue are dark and much more homogenous rectangular. This is caused by the salt, which is incorporated in the matrix crystals on the tissue surface [21]. Still, the unwashed tissue resulted in a rich MALDI spectrum after covering with the DHB matrix. After drying of the tissue sections, 4 nm of gold is deposited on top of the matrix crystals in order to prevent charging of the surface. Prevention of surface charging helps the analysis in two ways: (1) because of the increased signal intensities observed, and (2) it prevents blurring of the stigmatic images. Charging of the surface causes blurring of the stigmatic ion-optical images, since the ion-optics are sensitive to small changes in the sample potential.

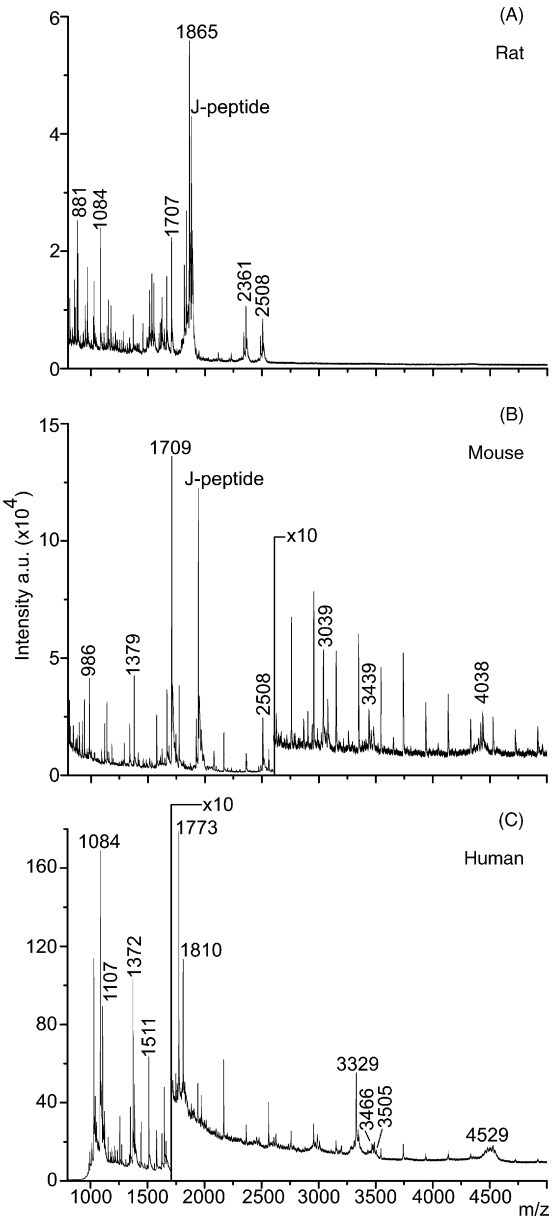

Fig. 2. MALDI-IMS spectra of mammalian pituitary tissue sections. Summed mass spectra of direct MALDI analysis of a: (A) HCCA covered rat pituitary, (B) DHB covered mouse pituitary and (C) HCCA covered human pituitary tissue section.

Table 1
Peptides from the MALDI-IMS analysis of rat, mouse and human pituitary and the FT-ICR analysis of the mouse pituitary tissue sections

Peptide	Rat pituitary		Mouse Pituitary				Human pituitary	
	IMS observed	IMS expected	IMS observed	IMS expected	FT-ICR observed*	FT-ICR expected*	IMS observed	IMS expected
ProOT/oxytocin (+Na)	1028.5*	1028.4					1029.6	1029.2
ProVP/vasopressin	1083.7*	1083.4					1084.3*	1083.4
POMC/des-Ac-α-MSH (5-13)							1154.6*	1154.6
ProVP/C-terminal fragment	1608.2	1607.8						
POMC/des-Ac-α-MSH	1623.4	1623.9	1624.2	1623.9			1623.9	1623.9
POMC/Ac-α-MSH	1665.5	1665.9	1666.3	1665.9	1664.813	1664.801		
POMC/diAc-α-MSH	1707.3	1708.0	1708.2	1708.0	1706.825	1706.811		
POMC/J-peptide (−18 Da)	1864.6							
POMC/J-peptide	1882.9	1883.9	1942.7	1942.0	1940.879	1940.863		
ProVP/C-terminal fragment	1948.2	1948.2						
POMC/Arg-CLIP (1–21)	2360.2	2360.6						
POMC/Arg-CLIP (1–22)	2507.3	2507.8	2507.9	2507.8	2506.297	2506.262		
POMC/Arg-CLIP (+Na)					2527.237	2527.260		
POMC/potential peptide							3006.9	3006.2
POMC/β-endorphin			3439.9	3438.1			3466.5	3466.1
POMC/Ac-β-endorphin			3479.8	3480.1			3505.0	3507.0

All observed masses in the MALDI-IMS analysis are average masses except for the ones marked with an asterisk (*). The asterisk represent that masses obtained in the FT-ICR experiment are all mono-isotopic.

3.3. Neuropeptide localization

Fig. 2 shows the summed mass spectra of rat (A), mouse (B) and human (C) pituitary tissue sections from IMS experiments. The spectra show a rich signature containing several peptides derived from the POMC precursor protein along with vasopressin at *m/z* 1084 and oxytocin at *m/z* 1028 (sodiated), derived from the ProVP and ProOX precursors, respectively. One of the POMC peptides, α-MSH is present in different degrees of acetylation (Table 1), with the most abundant form being diacetylated α-MSH in the spectra from mouse and rat. It is known from literature that the degree of acetylation plays a role in the potency of the neuropeptide [22,23]. Other POMC peptides seen in the spectra are the joining (J) peptide and corticotropin-like intermediary peptide (CLIP) and a CLIP fragment, POMC potential peptide and β-endorphin.

The mass spectra of the three pituitary tissue sections show clear differences from each other. In the mass spectrum of the mouse pituitary the vasopressin signal is absent, which can be explained by the absence of the neurohypophysis in the mouse pituitary tissue section. More importantly, the abundant J-peptide peak is not present in the mass spectrum of the human pituitary tissue, since this peptide is absent in the human POMC sequence. The POMC amino acid sequences in mouse, rat and human differ from each other by multiple amino acid substitutions. The molecular weight of the POMC protein in mouse, rat and human is 26,707, 26,540 and 29,424 Da, respectively, showing the largest difference exists between the human protein compared to the ones from mouse and rat. For this reason similar processing steps in the different organisms may lead to peptides with small differences in their amino acid sequence and thus in their mass. For example the amino acid sequence of β-endorphin in rat (YGGFMTSEKSQTPLVTLFKNAIIKNVHKKGQ, mass 3463.86) differs one amino acid from the sequence in mice (YGGFMTSEKSQTPLVTLFKNAIIKNAHKKGQ, mass 3435.83) and three amino acids from the β-endorphin sequence in humans (YGGFMTSEKSQTPLVTLFKNAIIKNAYKKGE, mass 3462.82). The before mentioned J-peptide, which differs 58 Da in mass between mouse and rat is even completely absent in humans. This phenomenon can be used to distinguish between different tissue types using IMS, where conventional imaging techniques like staining or fluorescence microscopy cannot. Furthermore, using MS the presence of amino acid substitutions are detected simultaneously with the imaging experiment itself. This demonstrates the possibility of IMS to reveal peptide or protein modifications directly from diseased tissue.

To verify the assignment of the observed peptides both LC–MS/MS and high mass accuracy MALDI FTICR-MS were used. In the LC–MS/MS experiment an extract of the rat pituitary was analyzed using a Q-ToF 2. Using this method, we were able to confirm the identity of peptides like vasopressin (data not shown). However, it is not trivial to elucidate the (endogenous) neuropeptide sequences from the masses observed in the imaging experiment using this technique. The use of a different ionization technique, electrospray versus MALDI, favors the ionization of different peptides and there are no databases available to identify endogenous neuropeptides on bases of their MS/MS spectra. To overcome these difficulties we used MALDI FTICR-MS, directly on mouse pituitary tissue sections to confirm the peptide assignments. Here the exact same sample preparation and ionization technique as in IMS can be used combined with high mass accuracy data analysis of the endogenous neuropeptides. Although the accurate mass analysis was enough to confirm the peptide assignments, we performed an infrared multiphoton dissociation (IRMPD) experiment on one of the peptides (J-peptide at *m/z* 1941) in the mouse pituitary. The resulting spectrum shows the expected fragments of the J-peptide and further helped in validating the assignment of the

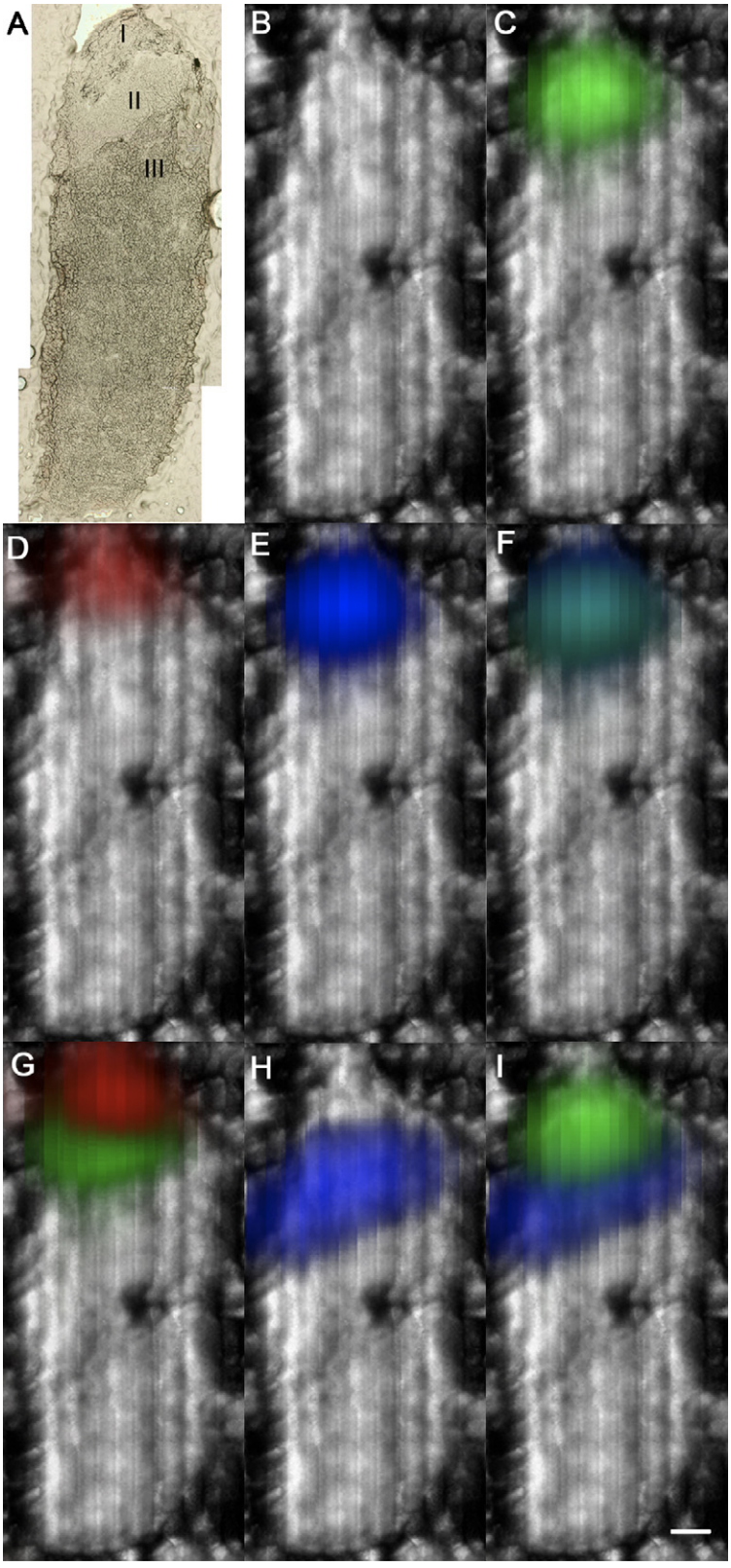

Fig. 3. Molecular imaging of rat pituitary tissue by MALDI-IMS. (A) Optical image of an untreated rat pituitary tissue section, with (I) the posterior lobe, (II) the intermediate lobe and (III) the anterior lobe. (B) TIC MALDI-IMS image in grayscale of a HCCA covered rat pituitary tissue section. (C) Distribution of the selected ion image of vasopressin (green), (D) oxytocin (red) and (E) C-terminal fragment of the ProVP precursor (blue) overlaid on the TIC image in grayscale. (F) Combined distributions of vasopressin (green) and the C-terminal fragment (blue) and (G) vasopressin (green) and oxytocin (red) overlaid on the TIC image in grayscale. (H) Distribution of the selected ion image of α-MSH (blue) and (I) combined distributions of vasopressin (green) α-MSH (blue) overlaid on the TIC image in grayscale. Scale bar is 200 μm.

peptides. Table 1 shows the assigned peaks from the different MS experiments. In the MALDI ToF spectra a lot of unidentified peaks remain and thus further tandem MS experiments are required to assign these peaks as well.

Fig. 3A shows an optical image of a pituitary gland from an adult rat. The rat pituitary consists of three distinct regions; the anterior, intermediate and posterior lobe. In Fig. 3B the stigmatic TIC image of the entire rat pituitary tissue section is shown in grayscale. Fig. 3C–I shows the MS images of the neuropeptide distributions in rat pituitary. In this experiment after each linescan the sample stage was moved upwards by 100 μm, resulting in a pixel size for the overlaid course *m/z* data of 10 μm × 100 μm. The images clearly show distinct localization of several endogenous neuropeptides in the different lobes of the pituitary. The POMC peptide α-MSH, in its different forms of acetylation, is localized in the intermediate pituitary where it is synthesized and secreted (H). The peptides vasopressin (C) and oxytocin (D) are localized in the posterior pituitary. A difference in localization can be seen between oxytocin and vasopressin within the same posterior pituitary (G), while signals derived from the ProVP precursor (E) at *m/z* 1610 (C-terminal fragment) and *m/z* 1947 (fragment 156–168) co-localize with the vasopressin signal (F). This result shows the ability to distinguish between clusters of different secretory cells within a ∼250 μm^2 area of the rat pituitary, using high spatial resolution imaging MS.

In the human pituitary tissue the peptide vasopressin is abundantly present, protonated and sodiated, as well as the sodiated form of oxytocin. α-MSH is only present in its des-acetylated form while β-endorphin can be found both with and without an acetyl group. Since the human pituitary is approximately 10

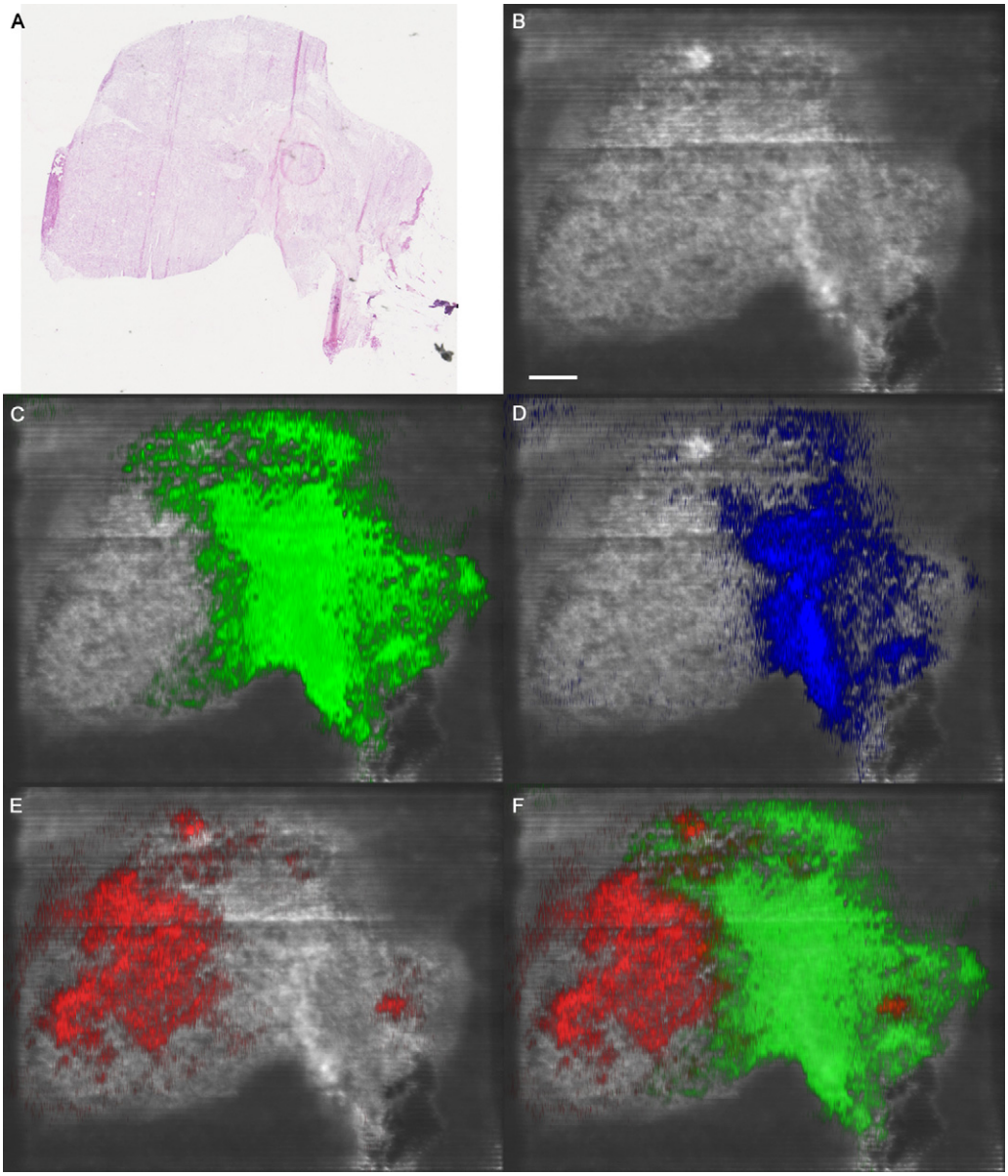

Fig. 4. Molecular imaging of human pituitary tissue by MALDI-IMS. (A) Optical image of an H&E stained human pituitary tissue section. (B) TIC MALDI-IMS image in grayscale of a tissue section adjacent to the one in the optical image. Neuropeptide distributions overlaid on the grayscale TIC image with (C) vasopressin in green (D) oxytocin in blue (E) α-MSH in red. (F) Overlay of vasopressin (green) and α-MSH (red). Scale bar is 1 mm.

times bigger than the mouse and rat pituitary, the signal intensity of the combined mass spectra is also ∼10 times higher.

Fig. 4A shows an optical image of a human pituitary tissue section. The tissue section comprises both the adenohypophysis (left) and the neurohypophysis (right). Fig. 4B shows the TIC image of the human pituitary tissue section. The contours and spatial details can again be clearly distinguished. Fig. 4C–F shows the molecular distribution of several neuropeptides in the human pituitary. The experiment was conducted in a similar fashion as in the case of the rat pituitary tissue, with the only difference being the distance between two linescans, which was 120 μm, resulting in a microprobe SIC pixel size of 10 μm × 120 μm. Both vasopressin (C) and oxytocin (D) nicely localize within the neurohypophysis and α-MSH in the adenohypophysis (E).

4. Conclusions

The high spatial resolution capability of the mass microscope allows localization of neuropeptides directly from tissue within tissue features at cell cluster length scales. In this approach either the combination of a high-resolution TIC background image with overlaid mass spectral data or high-resolution single ion microscope images can be obtained with the latter showing unprecedented detail with pixel sizes of 500 nm and resolving power of 4 μm. The sample preparation used to obtain the high-resolution images did not lead to diffusion of the analytes within or from the tissue. MS is able to distinguish different types of mammalian tissue based on the presence of differences in amino acid sequences of (neuro)peptides with similar function. This feature gives IMS an advantage over conventional imaging techniques in that it is able to look for small peptide or protein modifications (amino acid substitutions and post-translational modifications) in diseased tissue without prior knowledge.

Acknowledgements

The authors thank Angelique Verlaan, for cutting of the human pituitary tissue sections, Dr. Jens Fuchser and Dr. Goekhan Baykut, for assisting with the MALDI FT-ICR-MS experiments and Ivo Klinkert for continued assistance with the imaging software tools. Part of this work was carried out in the context of the Virtual Laboratory for e-Science project (www.vl-e.nl) and was supported by a BSIK grant from the Dutch Ministry of Education, Culture and Science (OC&W), part of the ICT innovation program of the Ministry of Economic Affairs (EZ). This imaging MS studies are part of the research program of the "Stichting voor Fundamenteel Onderzoek der Materie (FOM)", which is financially supported by the "Nederlandse organisatie voor Wetenschappelijk Onderzoek (NWO)".

References

[1] M. Stoeckli, P. Chaurand, D.E. Hallahan, R.M. Caprioli, Nat. Med. 7 (2001) 493.
[2] J. Pierson, J.L. Norris, H.R. Aerni, P. Svenningsson, R.M. Caprioli, P.E. Andren, et al., J. Proteome Res. 3 (2004) 289.
[3] P. Chaurand, S.A. Schwartz, R.M. Caprioli, Anal. Chem. 76 (2004) 86a.
[4] J. Pierson, P. Svenningsson, R.M. Caprioli, P.E. Andren, J. Proteome Res. 4 (2005) 223.
[5] K. Skold, M. Svensson, A. Nilsson, X. Zhang, K. Nydahl, R.M. Caprioli, P. Svenningsson, P.E. Andren, et al., J. Proteome Res. 5 (2006) 262.
[6] A.F.M. Altelaar, I. Klinkert, K. Jalink, R.P.J. deLange, R.A.H. Adan, R.M.A. Heeren, S.R. Piersma, et al., Anal. Chem. 78 (2006) 734.
[7] P. Chaurand, R.M. Caprioli, Electrophoresis 23 (2002) 3125.
[8] B. Spengler, M. Hubert, J. Am. Soc. Mass Spectrom. 13 (2002) 735.
[9] K.E. Schriver, P. Chaurand, R.M. Caprioli, 51st ASMS Conference, Montreal, 2003.
[10] S.L. Luxembourg, T.H. Mize, L.A. McDonnell, R.M.A. Heeren, Anal. Chem. 76 (2004) 5339.
[11] S.L. Luxembourg, L.A. McDonnell, T.H. Mize, R.M.A. Heeren, J. Proteome Res. 4 (2005) 671.
[12] H.-R. Aerni, D.S. Cornett, R.M. Caprioli, Anal. Chem. 78 (2006) 827.
[13] P.A. van Veelen, C.R. Jimenez, K.W. Li, W.C. Wildering, W.P.M. Geraerts, U.R. Tjaden, J. Van Der Greef, et al., Org. Mass Spectrom. 28 (1993) 1542.
[14] C.R. Jimenez, P.A. van Veelen, K.W. Li, W.C. Wildering, W.P.M. Geraerts, U.R. Tjaden, J. Van Der Greef, et al., J. Neurochem. 62 (1994) 404.
[15] R.M. Caprioli, T.B. Farmer, J. Gile, Anal. Chem. 69 (1997) 4751.
[16] G.T. Ooi, N. Tawadros, R.M. Escalona, Mol. Cell. Endocrinol. 228 (2004) 1.
[17] J.I. Young, V. Otero, M.G. Cerdan, T.L. Falzone, E.C. Chan, M.J. Low, M. Rubinstein, et al., J. Neurosci. 18 (1998) 6631.
[18] L.E. Pritchard, A.V. Turnbull, A. White, J. Endocrinol. 172 (2002) 411.
[19] S.A. Schwartz, M.L. Reyzer, R.M. Caprioli, J. Mass Spectrom. 38 (2003) 699.
[20] B.W. Schueler, Microsc. Microanal. Microstruct. 3 (1992) 119.
[21] S.L. Luxembourg, L.A. McDonnell, M.C. Duursma, X.H. Guo, R.M.A. Heeren, Anal. Chem. 75 (2003) 2333.
[22] D. Rudman, B.M. Hollins, M.H. Kutner, S.D. Moffitt, M.J. Lynn, Am. J. Physiol. Endocrinol. Metab. 245 (1983) E47.
[23] R.J. Arends, J. Rotllant, J.R. Metz, J.M. Mancera, S.E.W. Bonga, G. Flik, et al., J. Endocrinol. 166 (2000) 427.